20th Australasian Fluid Mechanics Conference
Perth, Australia
5-8 December 2016

Three-dimensional Vorticity Field behind two Side-by-Side Circular Cylinders in an Oblique Flow

T. Zhou[1], S. F. Mohd. Razali[2], , H. Wang[3] and Y. Zhou[4]

[1]School of Civil, Environmental and Mining Engineering
The University of Western Australia, 35 Stirling Highway, WA 6009, Australia

[2]Department of Civil and Structural Engineering, Faculty of Engineering and Built Environment, Universiti Kebangsaan Malaysia, 43600 UKM Bangi, Selangor, Malaysia.

[3]School of Civil Engineering and Architecture
Central South University, ChangSha, China

[4]Institute for Turbulence-Noise-Vibration Interaction and Control, Shen Zhen Graduate School, Harbin Institute of Technology, P R China

Abstract

Wake flows behind two side-by-side cylinders are investigated using an eight-hotwire vorticity probe in the intermediate region at four yaw angles (α), namely, 0°, 15°, 30° and 45° and for two centre-to-centre cylinder spacing ratios T^*, i.e., 3.0 and 1.7. For $T^* = 3.0$, there exist two vortex streets and the cylinders behave as independent and isolated ones. When $\alpha < 40°$, the independence principle (IP) is applicable in terms of the Strouhal number. The maximum coherent streamwise vorticity contours $\tilde{\omega}_x^*$ is only about 10% of that of the spanwise component $\tilde{\omega}_z^*$. With the increase of α, $\tilde{\omega}_x^*$ increases while $\tilde{\omega}_z^*$ decreases. At $\alpha = 45°$, $\tilde{\omega}_x^*$ is about 67% of $\tilde{\omega}_z^*$, indicating the existence of the secondary axial vortices with an enhanced three-dimensionality at larger α. For $T^* = 1.7$, only a single peak is detected in the energy spectrum ϕ_v. The IP is also applicable in the wake at this spacing ratio when $\alpha < 40°$. The vorticity contours for $T^* = 1.7$ at $\alpha = 0°$ have a more apparently organized pattern than that at large yaw angles. However, these contours are still much less organized and are much weaker in comparison with those for $T^* = 3.0$, indicating that the vortex motion in the wake when $T^* = 1.7$ is not stable.

Introduction

When a fluid flows over a bluff body at a sufficiently high Reynolds number Re ($\equiv U_\infty d/\nu$, where U_∞ is the free-stream velocity in the streamwise direction, d is the cylinder diameter and ν is the kinematic viscosity of the fluid), vortex shedding occurs, which results in a time-dependent pressure distribution on the solid surface. Vortex shedding from a single cylinder wake is well documented both in air and water flows. However, in the case when a fluid flows over two identical cylinders, the wake flow is far more complex than that of the single cylinder. Over the past decades, many researchers have contributed to the understanding of the flow around side-by-side cylinders [9]. Previous studies showed that this kind of flow depends not only on Re, but also on centre-to-centre cylinder spacing T^* (hereafter, an asterisk denotes normalization by the diameter d and/or the free-stream velocity U_∞). Various flow patterns have been identified as the cylinder spacing T^* is varied. At large cylinder spacing ($T^* \geq 2$), two coupled vortex streets have been observed with a definite phase relationship [2]. At intermediate cylinder spacing, $1.2 < T^* < 2.0$, the flow revealed two bi-stable wakes, one narrow and the other wide. The flow was flip-flopping and randomly changed from one side to the other because of the bi-stable deflected flow between the cylinders [1,3]. Sumner et al. [7] showed that at $T^* < 1.2$, the two side-by-side circular cylinders generate a single vortex street which is similar to that of a single one. However, the peak frequency in the power spectrum of the former is lower than that of the latter.

The previous studies focused only on the cross-flow case where the cylinder is perpendicular to the on-coming flow. In practical engineering applications, the cylinders may be yawed to the on-coming flow. In the present study, the yaw angle is defined as the angle between the incoming flow direction and the direction which is perpendicular to the cylinder axis (see Figure 1a). Flow structures and vortex shedding characteristics for a single yawed circular cylinder have been studied previously [8,11,6]. It has been shown that the vortex shedding frequency behaves in a similar way to a normal-incidence case through the use of the velocity component normal to the cylinder axis. If the force coefficients and the Strouhal number are normalized by the velocity component normal to the cylinder axis (i.e. $C_D = \frac{F_x}{0.5\rho U_N^2 A}$ and $St_N \equiv f_0 d/U_N$, where F_x is the force on the cylinder in the x-direction, ρ is the density of the fluid, A is the area projected on a vertical plane, f_0 is the vortex shedding frequency and $U_N \equiv U_\infty \cos\alpha$), the values are approximately independent of α. This is often known as the independence principle (IP) or the Cosine Law in the literature. Several theoretical and experimental studies have verified the IP. However, many studies showed deviations from the IP, especially at large yaw angles.

Experimental Details

The experiments were conducted in a closed loop wind tunnel with test section of 1.2 m (width) × 0.8 m (height) and 2 m in length. The free-stream velocity was 8.5 m/s (i.e. Re ≈ 7200) and the free-stream turbulence intensity was less than 0.5%. Two identical circular cylinders arranged side-by-side with a diameter d = 12.7 mm were used as wake generators. Two lateral spacings between the cylinders, namely $T^* = 3.0$ and 1.7, were tested. For each case, four yaw angles, α = 0°, 15°, 30° and 45°, were tested at a downstream location $x^* = 10$. The arrangement of the cylinder, the definition of the coordinate system and the sketches of the vorticity probe are shown in Figure 1. The vorticity probe was moved across the wake along the y-direction to measure simultaneously the three-dimensional vorticity. Another X-probe was fixed at $y^* = 4$-7 as a reference probe to provide a phase reference for the measured signals. Details of the vorticity probe can be found in [13].

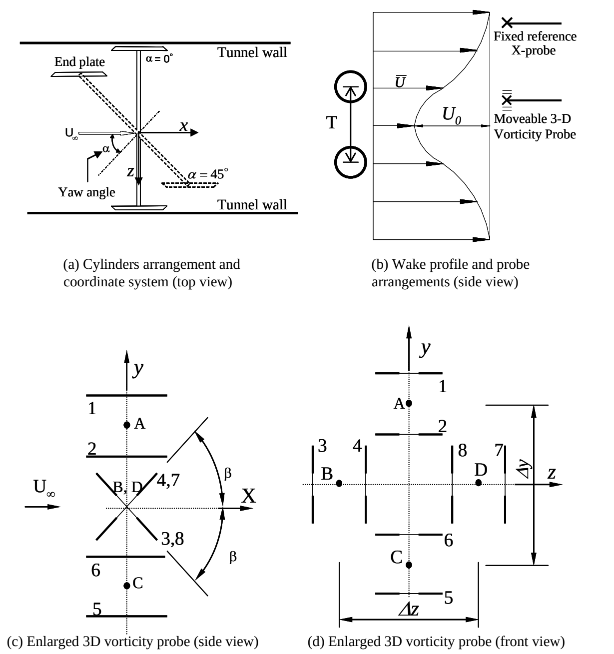

Figure 1. Two cylinders in side-by-side arrangement with definitions of the coordinate system and the sketches of the vorticity probe.

Results and Discussion

The energy spectra for α = 0° and 45° measured at y^* = 1.5 are shown in Figure 2. The results at α = 15° and 30° are not shown here as the spectra at these angles follow the trend when α varies from 0° to 45°. All power spectra are normalized to decibel scale by using the maximum of ϕ_v at α = 0° and 45°, respectively. The *x*-axis is normalized to f_N ($\equiv fd/U_N$). This normalization allows the peak frequency f_0 to correspond to the Strouhal number St_N ($\equiv f_0 d/U_N$). For T^* = 3.0 at α = 0° (Figure 2(a)), each power spectrum of all velocity components *u*, v and *w* shows a discernible peak which corresponds to St_N = 0.205. The peak energy of ϕ_v is the highest, followed by ϕ_u and ϕ_w. The St_N for T^* = 3.0 is comparable to that for a single cylinder at all yaw angles. With the increase of α to 45° (Figure 2(b)), the peak on spectra is broadening. For T* = 1.7, the energy spectrum for α = 0° (Figure 2(c)) shows a dominant peak occurring at St_N = 0.118. Chen et al. [2] detected two peaks in the spectra near 0.16 and 0.24 in their study for T^* = 1.7. The two peaks represent the Strouhal numbers for the wide and the narrow wakes. The wide wake has a lower Strouhal number while the narrow wake has a higher Strouhal number. Zhou et al. [12] also reported a single dominant frequency across the wake, which corresponds to St_N = 0.11. With the increase of α from 0° to 45°, the spectra exhibit a broad peak at a frequency which corresponds to St_N = 0.133, indicating that vortex shedding for α = 45° and T^* = 1.7 is not as apparent as that for α = 0° at T^* = 1.7 (Figure 2(c)) and for α = 45° at T^* = 3.0 (Figure 2(b)).

To examine the validity of IP, St_N at various yaw angles for T^* = 3.0 and 1.7 are compared in Figure 3 in terms of the ratio St_N/St_0 (where St_0 represents the Strouhal number at α = 0°). The results show that if a tolerance of ±8% is applied, the data support the IP for α < 40°. While for larger values of α, the difference of St_N/St_0 from 1 is far from the experimental uncertainty, suggesting a genuine departure from the IP. These variations indicate that the independence principle is also applicable to side-by-side cylinders with T^* = 3.0 an 1.7 when α < 40°.

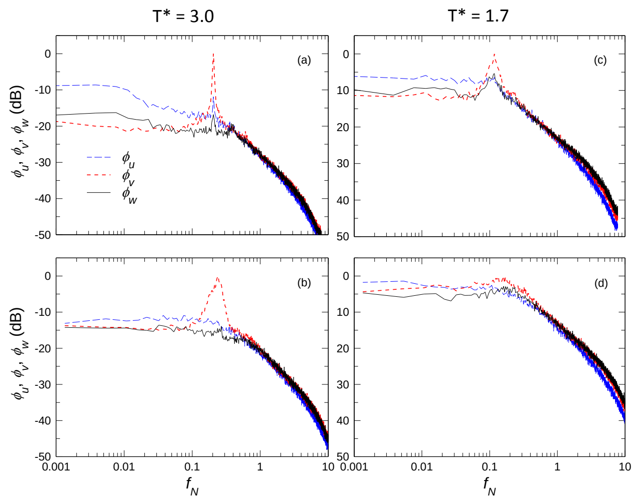

Figure 2. The power spectra of *u*, *v* and *w* components for different cylinder spacings at (a, c): α = 0°; (b, d): 45°.

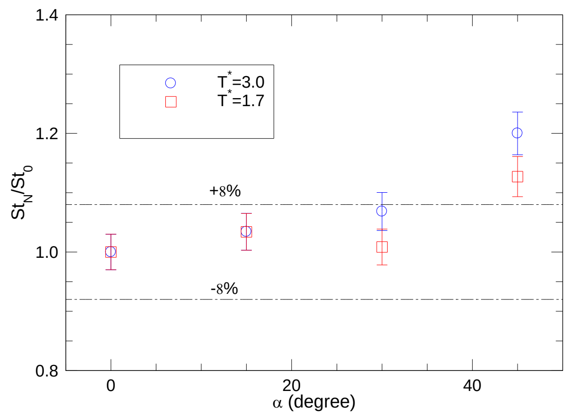

Figure 3. Strouhal number St_N for different cylinder spacing. The horizontal short dashed lines represent the range of experimental uncertainty

The near wake of a cylinder is characterised by apparent vortex shedding as reflected in Figure 2. With this shedding frequency, phase-averaged analysis can be conducted. Details of this method can be found in [13]. The phase-averaged spanwise vorticity contours for T^* = 3.0 (Figure 4(i-l)) display remarkable periodicity, resulting from the Kármán vortex street for all yaw angles. The contours are symmetric with respect to y^* = 0. At all yaw angles, the vorticity contours display two distinct vortex streets and the magnitudes of the contours are smaller than those for $T^* = \infty$ [13]. Here, only a single vortex street is shown as the wake is symmetric about y^* = 0. Another vortex street is located below the centreline. The spanwise vortex centres at α = 0° for T^* = 3.0 are around y^* = 1.3 and 1.9 for positive and negative vortices, respectively, while those for $T^* = \infty$ are around y^* = –0.2 and 0.4 [13]. It seems that if the whole set of the phase-averaged vorticity contours for T^* = 3.0 is allowed to shift downward by about y^* = 1.5, the vortex contours are quite similar with those for $T^* = \infty$ (figure is shown in [13]). These results affirm that the wake of two cylinders for T^* = 3.0 acts as two single-cylinder wake since it has similar vortex patterns as those for $T^* = \infty$. The maximum coherent spanwise vortices at α = 0° for T^* = 3.0 is 0.7 (Figure 4(i)). Even though there is a small decrease in the maximum contour values of $\tilde{\omega}_z^*$ when α varies from 0° to 30°, the variation is not very apparent. When α further increases to 45°, the maximum value of $\tilde{\omega}_z^*$ decreases by about 50%. This observation suggests that the effect of yaw angle on the coherent spanwise vortex is greater when α > 30°. This may be caused by the increase of the spanwise velocity $\bar{W}$ as α increases.

The streamwise vorticity contours for T^* = 3.0 exhibits organized patterns at all yaw angles. However, their strength are much weaker compared to those of $\tilde{\omega}_z^*$. At α = 0°, the size of the longitudinal vortices is much smaller than that of the spanwise vortices. The maximum magnitude of $\tilde{\omega}_x^*$ at this yaw angle is only about 7% of that of $\tilde{\omega}_z^*$, which is in agreement with the quisi-two-dimensionality of the flow. With the increase of yaw angles, the $\tilde{\omega}_x^*$ contours exhibit more apparently organised patterns and the maximum contour value increases monotonously. At α = 45°, the maximum contour value of $\tilde{\omega}_x^*$ (Figure 4(d)) is about 67% of that of $\tilde{\omega}_z^*$ (Figure 4(l)). This result indicates the existence of the secondary axial vortices with an enhanced three-dimensionality when α increases, consistent with the result for a single cylinder wake [13].

The coherent vorticity contours for T^* = 1.7 are shown in Figure 5. All vorticity contours for this spacing obviously have distinctly different vortex patterns from the aforementioned wakes for T^* = 3.0. Evidently, the wake for T^* = 1.7 has a larger vortex wavelength compared with that for T^* = 3.0. It can be seen that a single vortex street was shed from the top cylinder in the range from y* ≈ –1 to 3. The vortex structures in the wake are deflected downward below the wake centreline creating a wide wake above the centreline. The lower part of the wake region y^* < –1 may not be so important as it is believed that the vortex structures shed from the bottom cylinder are already vanished before x^* = 10 [2,12]. The formation of the vortex street in the wide wake at large downstream region is also illustrated and briefly discussed by Chen et al.[2] through numerical simulations for T^* = 1.7 at low Reynolds number (Re=750). They proposed the mechanisms involved in the vortex evolution of the wide and narrow wakes across the downstream region. Initially, the flow was deflected upwards creating a narrow wake around the top cylinder. The vortices in the narrow wake tend to pair and absorb the vortex from the bottom cylinder. Due to strong interaction between both vortices, the vortex shed from the bottom cylinder collapsed, thus encouraging the growth of the vortex from the top cylinder. As the vortex from the narrow wake (top cylinder) tends to prevent the merging of the following vortex from the wide wake (bottom cylinder), another vortex was created behind the bottom cylinder (now called a narrow wake). However, the vortex also collapsed quickly. At the same time, the vortex from the top cylinder become stronger and the flow deflected toward the bottom cylinder creating a wide wake. Finally, a single vortex street was formed in the wide wake at x^* = 10, which is consistent with the present results as shown in Figure 5. These mechanisms also explained the bi-stable deflected and flip-flopped flows with randomly changes from one side to the other as observed by [1,3,4]. Further observation by Zhou et al. [12] for two side-by-side cylinders for T^* = 1.5 at x^* = 10 shows that a row of weak vortices and another peculiar flow pattern are apparent. Such a peculiar flow pattern is diminished after x^* = 20, suggesting that the vortex regeneration or evolution is probably completed [12]. The two-cylinder case for T^* = 1.7 should bear a resemblance to that for T^* = 1.5 as they are in the same regime of the intermediate cylinder spacing (T^* = 1.2-2.0).

While the vorticity contours for T^* = 1.7 have a relatively more organised vortex pattern at α = 0°, it becomes scattered with the increase of the yaw angle. The maximum values of the $\tilde{\omega}_z^*$ contours are 0.14, 0.08, 0.08 and 0.06 at α = 0°, 15°, 30° and 45°, respectively. The values reveal a roughly decreasing trend as α is increased, especially when α = 45°. The unorganized vortex pattern of the $\tilde{\omega}_z^*$ contours may suggest that the vortex in the wake region of x^* = 10 is still not stable. This may support the flow visualization results by Williamson [9] behind two side-by-side cylinders for T^* = 1.5, who showed that the vortex regeneration or evolution may not be complete yet at x^* = 10. There is also another speculation that the vortices in the narrow wake have coalesced with those in the wide wake [12]. In comparison of the contours of $\tilde{\omega}_x^*$, $\tilde{\omega}_y^*$ and $\tilde{\omega}_z^*$, it is obvious that the magnitudes of all coherent vorticity components at each yaw angle are comparable (ranging from 0.06 to 0.12), indicating a more three-dimensional characteristic of the flow. With increasing α, the maximum values of the contours for $\tilde{\omega}_y^*$ and $\tilde{\omega}_z^*$ tend to be comparable, especially when α = 30° and 45°. This confirms that the transverse and spanwise vorticities are likely to have similar magnitudes and strength when α is increased to large yaw angles. When α = 45°, the maximum values of the $\tilde{\omega}_x^*$, $\tilde{\omega}_y^*$ and $\tilde{\omega}_z^*$ contours are similar (≈ 0.06). This shows that at large yaw angles, the vortices have strongly three-dimensional vortices as the strengths of vortices for all components are close to each other. While there is an apparent dependence of $\tilde{\omega}_z^*$ on α, which decays by 50% when α is increased from 0° to 45°, the increase of $\tilde{\omega}_x^*$ with α for T^* = 1.7 is not as apparent as that for T^* = 3.0. This result indicates a strong interaction between the wake structures when T^* = 1.7.

Conclusions

Experiments of two side-by-side cylinders with T* = 3.0 and 1.7 and α = 0°, 15°, 30° and 45° have been conducted to evaluate the characteristics of vortex shedding. For T^* = 3.0, a single peak is observed on the spectra of ϕ_V. For α < 40°, the independence principle is applicable to the wake. The phase-averaged vorticity contours for T^* = 3.0 are comparable with those for T^* = ∞. This result confirms that the wake of two side-by-side cylinders for large cylinder spacing, i.e. T^* = 3.0 behaves as an independent and isolated cylinder. The coherent streamwise vorticity contours $\tilde{\omega}_x^*$ for T^* = 3.0 is only about 10% of that of the coherent spanwise vorticity contours $\tilde{\omega}_z^*$. With the increase of α, $\tilde{\omega}_x^*$ increases while $\tilde{\omega}_z^*$ decreases. At α = 45°, $\tilde{\omega}_x^*$ is about 67% of $\tilde{\omega}_z^*$. This result indicates the existence of the secondary axial vortices with an enhanced three-dimensionality with large α.

For intermediate cylinder spacing T^* = 1.7, only a single peak is detected on the energy spectra ϕ_V. This is because at x^* = 10, the vortex structure regeneration or evolution may not be completed yet, whereas those in the narrow wake are probably diminished before the downstream location. The independence principle (IP) is applicable to the wake when α < 40°. The vorticity contours for T^* = 1.7 have a more organized pattern at α = 0° while become scattered and smaller with the increase of the yaw angles. With increasing α, there is a decreasing trend in the maximum value of vorticity contours. The less organized $\tilde{\omega}_z^*$ contours for T^* = 1.7 compared with those for T^* = ∞ and 3.0 indicate that the vortex motion in the wake is still not stable, suggesting that the vortex evolution or regeneration process may not be completed yet. At α = 45°, the vortices show apparent three-dimensionality as the strengths of all vortices are the same. The maximum contours of the coherent vorticity components $\tilde{\omega}_x^*$ and $\tilde{\omega}_z^*$ for T^* = 1.7 are about 30% and 7% of those for T^* = 3.0. These results suggest that the coherent vorticity components for T^* = 1.7 are much weaker than that of both T^* = 3.0 and a single cylinder wake.

References

[1] Bearman, P.W. & A.J. Wadcock, The interaction between a pair of circular cylinders normal to a stream, *Journal of Fluid Mechanics*, 61, 1973, 499-511.

[2] Chen, L., Tu, J.Y. & Yeoh, G.H., Numerical simulation of turbulent wake flows behind two side-by-side cylinders, *Journal of Fluids and Structures*, 18, 2003, 387-403.

[3] Ishigai, S., Nishikawa, E., Nishimura, K. & Cho, K., Experimental study on structure of gas flow on tube banks with tube axes normal to flow (Part 1, Karman vortex flow from two tubes at various spacings), *Bulletin of Japan Society of Mechanical Engineers*, 15, 1972, 945-956.

[4] Kim, H.J. & Durbin, P.A., Investigation of the flow between a pair of circular cylinders in the flopping regime, *Journal of Fluid Mechanics*, 196, 1988, 431-448.

[5] Lucor, D. & Karniadakis, G.E., Effects of oblique inflow in vortex-induced vibrations, *Flow, Turbulence and Combustion*, 71, 2003, 375-389.

[6] Marshall, J.S., Wake dynamic of a yawed cylinder, *Journal of Fluids Engineering*, 125, 2003, 97-103.

[7] Sumner, D., Wong, S.S.T., Price, S.J. &Païdoussis, M.P., Fluid behaviour of side-by-side circular cylinders in steady cross-flow, *Journal of Fluids and Structures*, 13, 1999, 309-338.

[8] Surry, D. & Surry, J., The effect of inclination on the Strouhal number and other wake properties of circular cylinders at subcritical Reynolds numbers, *in Technical Report. UTIAS TechnicaI Institute for Aerospace Studies*, University of Toronto, 1967.

[9] Williamson, C.H.K., Evolution of a single wake behind a pair of bluff bodies, *Journal of Fluid Mechanics*, 159, 1985, 1-18.

[10] Zdravkovich, M.M., Review of flow interference between two circular cylinders in various arrangements, *Journal of Fluids Engineering*, 99, 1977, 618-633.

[11] Zhou, T., Razali, S.F.M., Zhou, Y., Chua, L.P. & Cheng, L., Dependence of the wake on inclination of a stationary cylinder, *Experiments in Fluids*, 46, 2009, 1125-1138.

[12] Zhou, Y., Zhang, H.J. & Yiu, M.W., The turbulent wake of two side-by-side circular cylinders, *Journal of Fluid Mechanics*, 458, 2002, 303-332.

[13] Zhou, T., Wang, H., Razali, S.F.M., Zhou, Y. & Cheng, L., Three-dimensional vorticity measurements in the wake of a yawed circular cylinder, *Physics of Fluids*, 22, 2010, 015108.

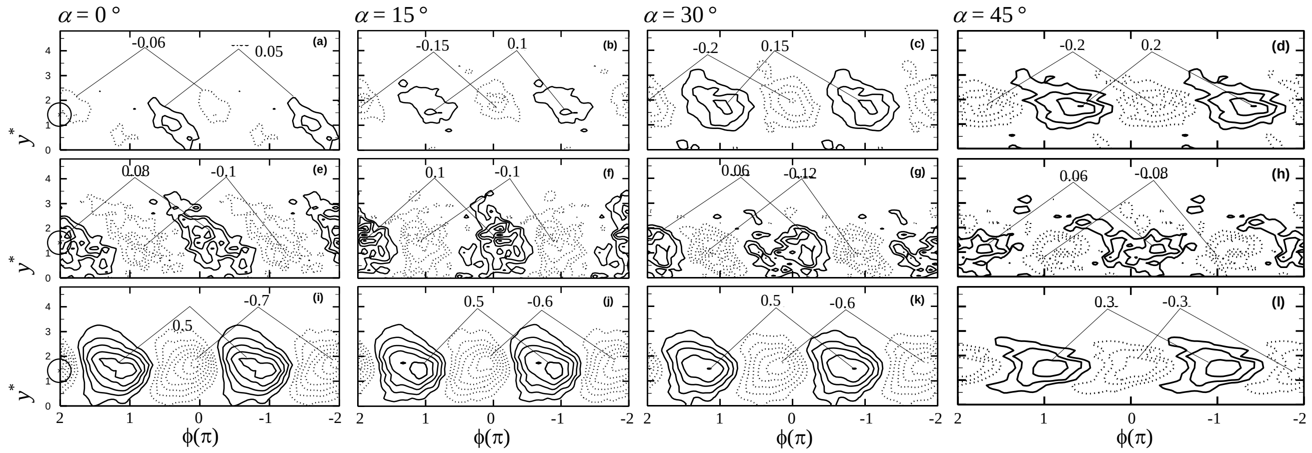

Figure 4. Phase-averaged vorticity components at different yaw angles for $T^* = 3.0$. (a-d) $\tilde{\omega}_x^*$; (e-h) $\tilde{\omega}_y^*$; (i-*l*) $\tilde{\omega}_z^*$. (a-d) Contour interval = 0.05; (e-h) 0.02; (i-*l*) 0.10. $\phi = 2\pi$ corresponds to the λ ($\equiv U_c/f_0$). The open circle with a cross at the centre ⊙ represents cylinder.

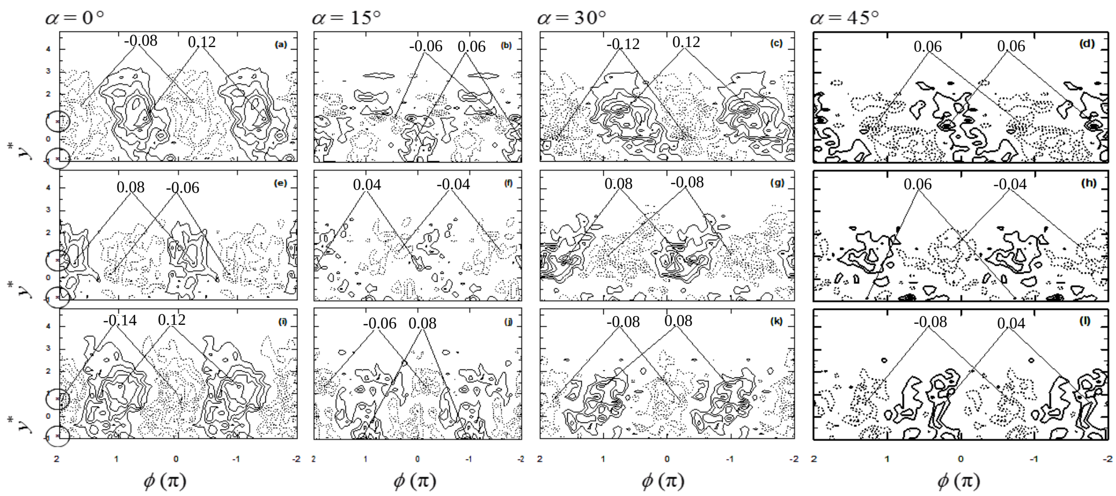

Figure 5. Phase-averaged vorticity components at different yaw angles for $T^* = 1.7$. (a-d) $\tilde{\omega}_x^*$; (e-h) $\tilde{\omega}_y^*$; (i-*l*) $\tilde{\omega}_z^*$. (a-*l*) Contour interval = 0.02. $\phi = 2\pi$ corresponds to the $\lambda/2$ ($\equiv U_c/2f_0$). The open circle with a cross at the centre ⊙ represents the cylinder.